Competition between Cure and Thermal Degradation in a High T_g Epoxy System: Effect of Time and Temperature of Isothermal Cure on the Glass Transition Temperature

K. P. PANG and J. K. GILLHAM, *Polymer Materials Program, Department of Chemical Engineering, Princeton University, Princeton, New Jersey 08544*

Synopsis

The isothermal cure of a diglycidyl ether of bisphenol A with a tetrafunctional aromatic diamine has been studied in an attempt to achieve full cure (maximum glass transition temperature, $T_{g\infty}$, ca. 170°C). Since high temperatures of cure are necessary for high $T_{g\infty}$ systems (because of low reaction rates after vitrification), cure and thermal degradation reactions often compete. In this work T_g is used as a direct measure of conversion. An approach leading to a series of iso-T_g contours in a temperature vs. time transformation (TTT) diagram, which can be used to design time–temperature cure paths leading to particular values of T_g, is discussed.

INTRODUCTION

Epoxy resins are widely employed as coatings and adhesives and in structural applications which require light weight and high strength. One of the major tasks in polymeric materials science is to understand how the molecular structure of a thermosetting material affects its macroscopic properties, which, in turn, govern its end-use performance.

During cure, low molecular weight liquid epoxy resin is transformed into a crosslinked polymeric glass or rubber by chemical reactions. A temperature (T_c) vs. time transformation (TTT) diagram,[1,2] as shown in Figure 1, provides an intellectual framework for understanding the process of isothermal cure of epoxy resins in terms of the different material states encountered; key parameters are defined in the caption to Figure 1. The material characteristics of a thermosetting polymer change during cure, both with time and temperature. The glass transition temperature (T_g), for example, can change from that of the reactants (T_{g0}), through that of the material at its chemical gelation point ($_{gel}T_g$), to that of the fully reacted product ($T_{g\infty}$). It is a prerequisite to obtain fully cured materials before definitive correlations between molecular structure and macroscopic properties can be achieved. However, to achieve full cure is not a trivial task because of the complexity of the cure process. The main cure reaction in the systems being investigated in this laboratory is the stoichiometric addition of epoxide and amine groups[3]; however, there are complicating factors. These include competitive epoxide homopolymeriza-

Journal of Applied Polymer Science, Vol. 39, 909–933 (1990)
 CCC 0021-8995/90/040909-25$04.00

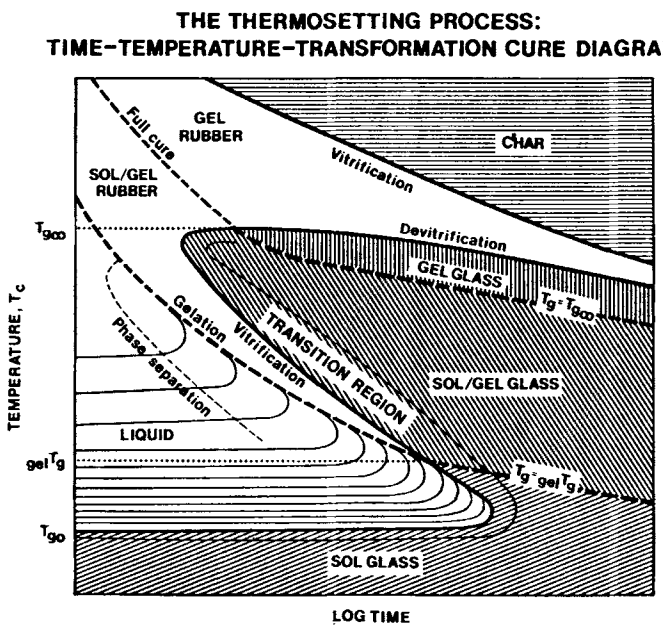

Fig. 1. Schematic isothermal time–temperature–transformation (TTT) cure diagram of a thermosetting polymer, displaying three characteristic temperatures ($T_{g\infty}$, $_{gel}T_g$, T_{g0}) and distinct regions of matter [liquid, sol/gel rubber, gel rubber, sol glass, sol/gel glass, fully cured (gel) glass, and char]. Successive isoviscous contours shown in the liquid region differ by a factor of 10. Phase separation, as in rubber-modified systems, occurs prior to gelation. Vitrification occurs when $T_g = T_c$. The full cure contour corresponds to $T_g = T_{g\infty}$. Degradation events are devitrification and char formation.

tion[4,5] and thermal degradation reactions[6,7] competing with cure at high temperatures,[8] as well as incomplete conversion due to diffusion-controlled reactions beyond gelation or vitrification[2,9,10] and topological constraints imposed by the crosslinked network as reactive groups are isolated during the reaction.[11] Consequently, although the molecular architecture and, therefore, the properties of a cured system can be varied by the reaction pathway, a well-defined molecular structure in general is not attainable. In particular, the intrinsic glass transition temperature at full cure may not be realizable.

This paper reports a characterization study of a difunctional epoxy/tetrafunctional aromatic amine system with a maximum T_g of about 170°C which addresses the following issues: (1) the effect of cure and thermal degradation on the material properties during and after isothermal cure, (2) the effectiveness of using T_g as an index of the progress of cure, and (3) the development of a methodology for obtaining the maximum value of T_g. The technique used for this report was principally torsional braid analysis (TBA),[1,2,12] which is a particularly convenient one for relating cure to properties. An earlier study [13] on the same difunctional epoxy system focused on isothermal cure temperatures (T_c) below 150°C. In this work, T_c's above 150°C were also investigated so that the effects of cure and thermal degradation on the glass transition temperature could be studied. A preliminary report has been published.[14]

EXPERIMENTAL

Materials

The difunctional epoxy monomer used for this report was a diglycidyl ether of bisphenol A (DGEBA) (DER 331, Dow Chemical Co.) cured with a tetrafunctional aromatic diamine, trimethylene glycol di-*p*-aminobenzoate ("TMAB," Polacure 740M, Polaroid Corp.)[8,13-16] The chemical formulae of the reactants are shown in Figure 2. The materials were reacted stoichiometrically, one epoxy group with one amine hydrogen, according to their respective equivalent weights: DER 331, 190 g/Eq; TMAB, 78.5 g/Eq.

The details for preparation of a master batch have been published.[14,16] For this report, a sample for torsional braid analysis was dissolved in methyl ethyl ketone (1 g solid/1 mL solvent). The solution was kept in a refrigerator for storage when not in use. All cure conditions were above the boiling point of the solvent (80°C).

Torsional Braid Analysis (TBA)

An automated torsional pendulum[1,12] provides the basis of a technique for monitoring the transitions (ca. 1 Hz) during the course of cure and, from subsequent temperature scans, the transitions after cure. The technique, TBA, uses an inert multifilamented glass braid impregnated with the reactive liquid as the easily made specimen. The pendulum is intermittently set into small angle free oscillations to generate a series of damped waves. Each wave is characterized by the frequency and the decay constants which are related to material behavior through two dynamic mechanical parameters, relative rigidity and logarithmic decrement. The relative rigidity, $1/P^2$, is related to the

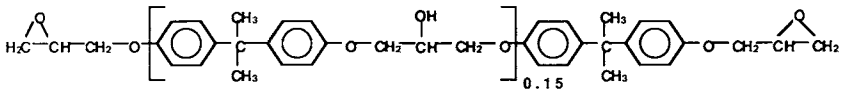

Diglycidyl Ether of Bisphenol A [DER 331]

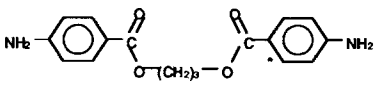

Trimethylene Glycol Di-p-aminobenzoate [TMAB]

Fig. 2. Chemical formulae of the reactants (DER 331/TMAB system).

elastic shear modulus G',

$$G' \simeq (8\pi IL/r^4)(1/P^2) \tag{1}$$

where r and L are the radius and length of the specimen, I is the moment of inertia of the oscillating system, and P is the period of oscillation. The logarithmic decrement is equal approximately to $\pi G''/G'$, where G'' is the loss shear modulus. Quantitative values of G' and G'' for the supported material are not obtained due to the composite nature of the TBA specimen. However, the times and temperatures of transitions, which are assigned from the maxima in mechanical damping, are easily measured.

During the course of cure, the relative rigidity, $1/P^2$, can vary as a result of both changing modulus and dimensions of the specimen. The volume of a specimen, V, can be approximated by that of a regular cylinder, i.e., $V = \pi r^2 L$. As $L/r \simeq 100$,

$$V = 100\pi r^3 \tag{2}$$

Using eqs. (1) and (2), the relative rigidity at two different states of cure can be compared:

$$(1/P^2)_2/(1/P^2)_1 = (G'r^4)_2/(G'r^4)_1 \tag{3}$$

$$V_2/V_1 = (r_2/r_1)^3 \tag{4}$$

where subscript 2 designates more advanced cure. Combining eqs. (3) and (4) yields

$$(1/P^2)_2/(1/P^2)_1 = (G'_2/G'_1)(V_2/V_1)^{4/3} \tag{5}$$

Since shrinkage is associated with the cure and degradation of epoxies (i.e., $V_2 < V_1$), the relative rigidity will actually decrease if not compensated by a corresponding increase in the modulus.

The times to macroscopic gelation and to vitrification are two important parameters for characterizing the cure of thermosetting systems. They were assigned from the times to consecutive maxima in each logarithmic decrement vs. time plot for each isothermal cure.[1,8,12–16] After isothermal cure at temperature T_c, the dynamic mechanical behavior in the temperature scan, $T_c \rightarrow -170 \rightarrow 240 \rightarrow -170$°C at 1.5°C/min, was used to identify transition temperatures from the maxima in each logarithmic decrement vs. temperature plot. The scan from -170 to 240°C yielded the glass transition temperature of the material cured at T_c; the subsequent scan from 240 to -170°C yielded the glass transition temperature of the postcured material. $T_{g\infty}$ is operationally defined in this work to be the maximum glass transition temperature obtained by isothermal cure. All TBA experiments were performed in dry helium; all heating and cooling rates were at 1.5°C/min.

The automated TBA torsion pendulum system is available from Plastics Analysis Instruments, Inc., P.O. Box 408, Princeton, NJ 08540.

RESULTS AND DISCUSSION

Cure, and Times to Transitions

A dynamic mechanical spectrum for the epoxy system during isothermal cure at 100°C (i.e., $T_c < T_{\infty}$) for 336 h is shown in Figure 3. The first transition is assigned to macroscopic gelation: $t_{gel} \simeq 401$ min. Similar methods for locating the macroscopic gel point have been used in the literature.[1,17-19] The second transition is assigned to vitrification, which occurs when the glass transition temperature rises to the cure temperature: $t_{vit} \simeq 729$ min. Since the relative rigidity does not "level off" until well after the assigned t_{vit}, a seemingly more appropriate indicator for defining the time for the material to be in the glassy state is that at which the relative rigidity has changed by less than, for example, $\pm 0.1\%$ during the preceding period of 10,000 min ($\equiv t_{glass}$), as indicated by the arrow in Figure 3. However, measurement of the parameter t_{glass} is less reproducible than locating the maximum in the logarithmic decrement. Further, as T_c approaches $T_{g\infty}$ the final state will not be glassy at T_c; for this reason Figure 4 shows data for t_{glass} for $T_c \leq T_{g\infty} - 30$°C, i.e., ≤ 140°C (see later). Similarly, t_{vit} measurements are valid only for $T_c \leq T_{g\infty}$. The time width of the isothermal vitrification process can be defined by $\Delta t_g = t_{glass} - t_{vit}$, which varies with T_c, as depicted in Figure 4 (which also includes data for t_{vit} and t_{glass}). Parameters Δt_g and t_{glass} exhibit a minimum at approximately 120°C, whereas t_{vit} exhibits a minimum at approximately 150°C. For t_{vit}, this can be explained in terms of simple kinetics analysis that is typical of an nth order reaction: The reaction rate increases with increasing T_c in terms of the rate constant, but decreases with increasing conversion. (The numerical values for Δt_g and t_{glass} are similar on a logarithmic scale because of the relatively low values of t_{vit}.) During and beyond vitrification process, the reaction becomes diffusion controlled.

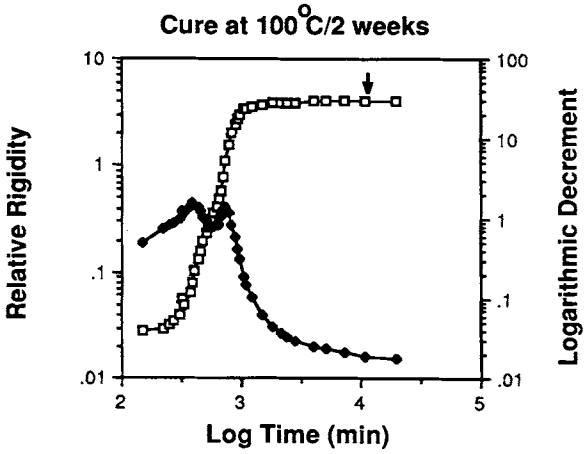

Fig. 3. Dynamic mechanical spectrum of isothermal cure at 100°C for 336 h (□) relative rigidity; (◆) logarithmic decrement. Vertical arrow defines t_{glass} (see text).

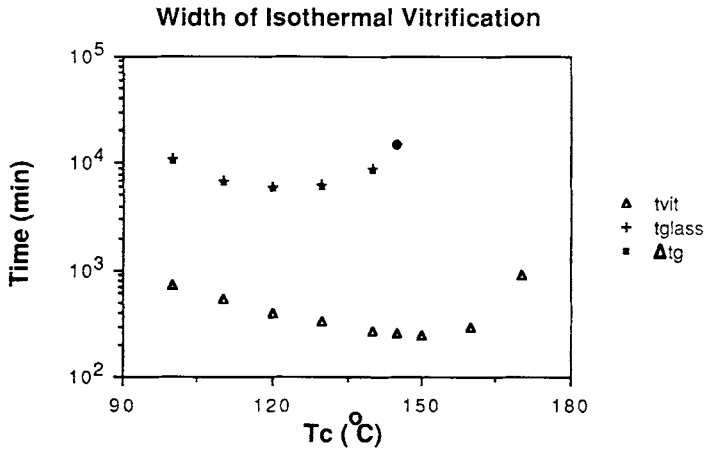

Fig. 4. t_{vit}, t_{glass}, and the width of the isothermal vitrification process (Δt_g) vs. T_c: (△) t_{vit}; (+) t_{glass}; (■) Δt_g.

During isothermal cure, the rigidity can plateau at a value which is less than that of the glassy state. Figure 5 shows plots of relative rigidity vs. log time from T_c = 100–240°C. Data for two or three different cure times (and therefore different composite specimens) at each T_c are included, without discriminating the data, to demonstrate the reproducibility and semiquantitative nature of the data. At long cure times, the relative rigidity at each T_c reaches a plateau, the value of which corresponds to the state of the material. It can be observed that the relative rigidity of the partially and "fully" crosslinked rubbery region (at all cure temperatures) can be demarcated within the dashed lines. At $T_c \simeq T_{g\infty}$, the plateau value lies between those of the glassy and the rubbery states. Hence for $T_c > T_{g\infty} - 30$°C (see later), t_{glass} cannot be defined. Figure 6 shows plots of logarithmic decrement vs. log time of cure for T_c = 100, 170, and 187°C (one set of cure data for each T_c is shown). As can be observed, the vitrification (second) peak is sharp at

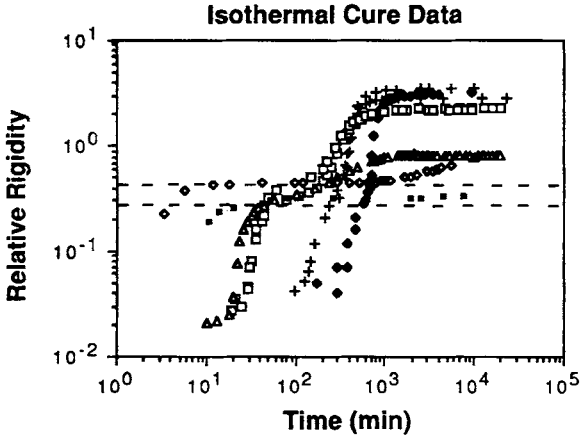

Fig. 5. Relative rigidity vs. log time of isothermal cure at various T_c's: (◆) 100°C; (+) 120°C; (□) 160°C; (△) 170°C; (■) 200°C; (◇) 240°C. The rubbery region: (= = =).

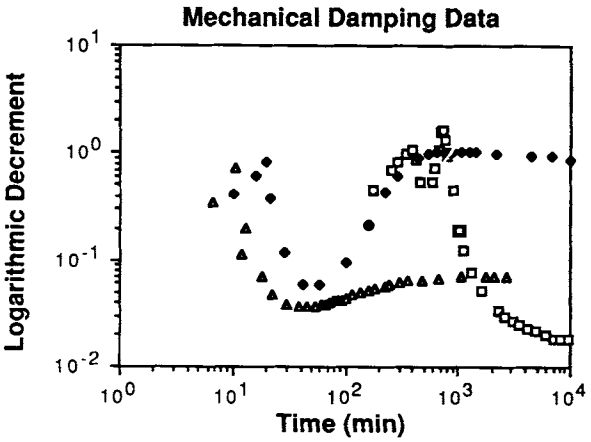

Fig. 6. Mechanical damping data. Logarithmic decrement vs. log time of isothermal cure at various T_c's: (□) 100°C; (◆) 170°C; (△) 187°C.

T_c = 100°C; it broadens, and its intensity decreases somewhat, as $T_c \rightarrow T_{g\infty}$. In the absence of thermal degradation, the damping level should rise to a constant level at T_c = 170°C which corresponds to that at the glass transition of the fully reacted material (cf. Fig. 10). Similarly the damping should rise to a constant level at T_c = 187°C, which, in a temperature scan, should correspond to a level of the logarithmic decrement of the fully reacted material above $T_{g\infty}$ at 187°C.

Thermal Degradation

Thermal degradation can occur in competition with cure when the epoxy system is cured at high temperatures. Figure 7 shows plots of relative rigidity and logarithmic decrement vs. log time for isothermal heating at 170, 220, and 240°C. At 170°C, after the assigned time to vitrification (a broad maximum in the logarithmic decrement), the relative rigidity continues to increase before reaching a maximum (as indicated by the solid arrow). The subsequent decrease in relative rigidity, which is apparently caused by thermal degradation, is also observed at lower T_c's (see Fig. 9). After a long time at 170°C the relative rigidity increases again (as indicated by the dashed arrow) in a process which is designated "char" formation. (In previous studies, the time to char formation was measured by a maximum in the logarithmic decrement.[8]) At 220 and 240°C, after macroscopic gelation (which occurs prior to measurement), the relative rigidity increases and then remains constant (which represents approximately full cure in the rubbery state) before increasing again after a long time (dashed arrows). The higher T_c, the shorter the time to the onset of char formation. In the rubbery state the modulus (relative rigidity) of fully cured rubber increases with temperature, in accordance with the theory of rubber elasticity.[20]

Figure 8 shows plots of relative rigidity and logarithmic decrement vs. reduced temperature, $(T - T_g)$, from T_g to 240°C for three specimens with different cure histories. When the material is either partially cured (100°C/70 h, T_g = 126.5°C) or "fully" cured (170°C/96 h, T_g = 169.5°C), the relative

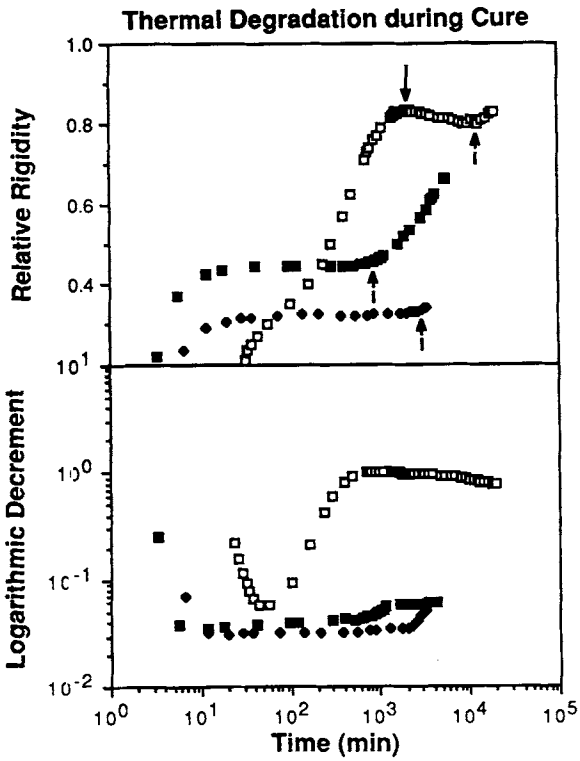

Fig. 7. Thermal degradation during cure. Relative rigidity (top) and logarithmic decrement (bottom) during isothermal heating: (□) 170°C; (◆) 220°C; (■) 240°C. Vertical solid arrow marks the time to reach a maximum relative rigidity. Vertical dashed arrows mark the onset of char formation.

rigidity is observed to increase with temperature in the rubbery state. This has also been shown for DGEBA systems[20,21] and for elastomers in general.[22] However, after isothermal heating at 240°C for 96 h (T_g = 165°C), the subsequent temperature scan depicts different behavior in the rubbery state—the relative rigidity decreases with increasing temperature. Similar behavior can be observed in the TBA data of previous studies on epoxy systems in which thermal degradation had occurred.[8] The behavior observed in Figure 8 may be related to the thermoelastic inversion phenomenon[23]; it suggests that thermal degradation produces a less strained condition in the rubbery state in comparison with normal cure. In addition, the damping level above T_g of the degraded material is higher, and the glass transition temperature is lower, than that of the normal fully crosslinked material.

The Isothermal TTT Diagram

The corresponding values of t_{gel}, t_{vit}, t_{glass}, and the time to the onset of char formation at each isothermal cure temperature are plotted in Figure 9 to give the macroscopic gelation, vitrification, glass, and onset of char formation contours, respectively, in the form of a TTT diagram. Also shown are the times to reach a maximum in the relative rigidity for $T_c < T_{g\infty}$. In general,

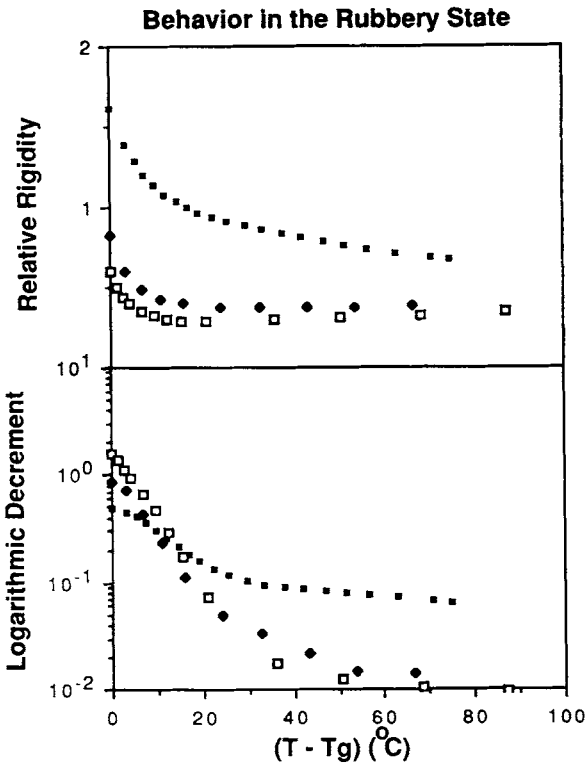

Fig. 8. Behavior in the rubbery state. Relative rigidity (top) and logarithmic decrement (bottom) vs. $(T - T_g)$ for specimens with different cure histories: (□) 100°C for 70 h; (◆) 170°C for 96 h; (■) 240°C for 96 h. Scanning rate: + 1.5°C/min in dry helium.

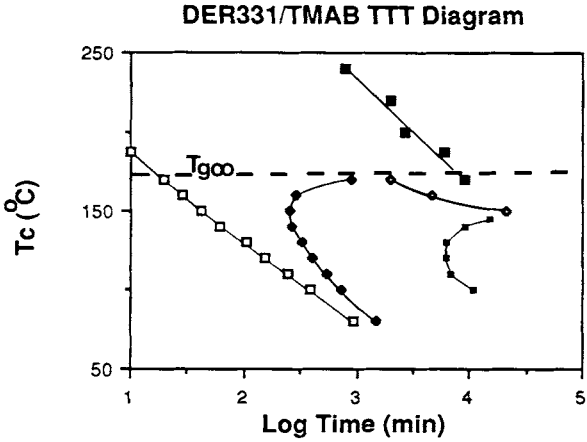

Fig. 9. DER 331/TMAB time–temperature–transformation (TTT) isothermal cure diagram: (□) macroscopic gelation; (◆) vitrification; (■) glass; (◊) maximum relative rigidity; (■) char formation. The maximum value of T_g obtained by isothermal cure $T_{g\infty} \simeq 170$°C.

only the part of the TTT cure diagram which is above $T_c = 80°C$ was obtained so as not to consider the presence of solvent (bp ca. 80°C) in the reactive liquid sample. The T_g of the unreacted solvent-free system as measured by differential scanning calorimetry (DSC) is ca. 13°C (T_{g0}; see Fig. 1)[24] (data not shown). Using the TTT diagram as a framework, isothermal cure paths have been designed to study the effect of time and temperature of cure on the glass transition temperature[13,14] and on material properties at room temperature.[15,16]

Temperature ${}_{gel}T_g$ (see Fig. 1), which has been defined as the temperature at which molecular gelation and macroscopic vitrification coincide for isothermal cure,[1,2,25] is the glass transition temperature of the material at the composition corresponding to gelation. [Being a glass transition temperature, it is time (frequency) dependent. In TBA work T_g, and therefore also vitrification, occur at approximately 0.7 Hz.] Values of ${}_{gel}T_g$ have been estimated from the intersection of the extrapolated logarithmic times to macroscopic gelation and to macroscopic vitrification vs. $1/T_c$ (K) for several DGEBA systems.[2] This temperature is defined as ${}_{gel}T_g'$. This procedure for the current system yields a value of 67°C for ${}_{gel}T_g'$. However, the data in Ref. 2 show that the time gap between macroscopic gelation and vitrification ($t_{vit} - t_{gel}$) actually increases with decreasing temperatures. The present results show that $t_{vit} - t_{gel}$ increases from 208 min at 140°C to 580 min at 100°C. Nevertheless, the time gap diminishes on a logarithmic time scale.

The molecular gel point occurs at a particular extent of reaction.[23] In contrast, rheological techniques measure macroscopic gelation, which is often measured as an isoviscous event[1]. If the TBA assignment of macroscopic gelation is of an isoviscous event and if the viscosity at vitrification is a higher value, then macroscopic gelation will occur prior to vitrification as long as the initial viscosity is lower than the isoviscosity level. Consequently, the two macroscopic events need not converge during isothermal cure at low temperatures.

Transitions

The temperature scan (Fig. 10) of the material from −170 to 240°C after cure at 100°C (i.e., $< T_{g\infty}$) for 336 h (Fig. 3) yields a T_g value of 131°C (ca. 0.7 Hz) as determined from the maximum in the logarithmic decrement. The assigned T_g is closer to the higher temperature end of the defined transition region (ΔT_g; between vertical arrows, Fig. 10). From the value of the relative rigidity at $T_c = 100°C$, the material is in the glassy state at the end of the isothermal cure (Fig. 3). As the width of the glass transition (ΔT_g) is about 42°C, it is not unusual that T_g as measured in this fashion is higher than T_c by about 30°C. This is the reason for limiting measurements of t_{glass} to $T_c \leq T_{g\infty} - 30°C$ (see earlier).

The subsequent scan from 240 to −170°C (Fig. 10) yields a value for T_g of 167.5°C (ca. 0.7 Hz). In general, the T_g (after post-cure to and from 240°C) measured in this manner is not a constant value (range: 165–170°C) as the degree of post-cure is different for materials with different thermal prehistories. This reflects that: (1) "full" cure cannot generally be achieved during

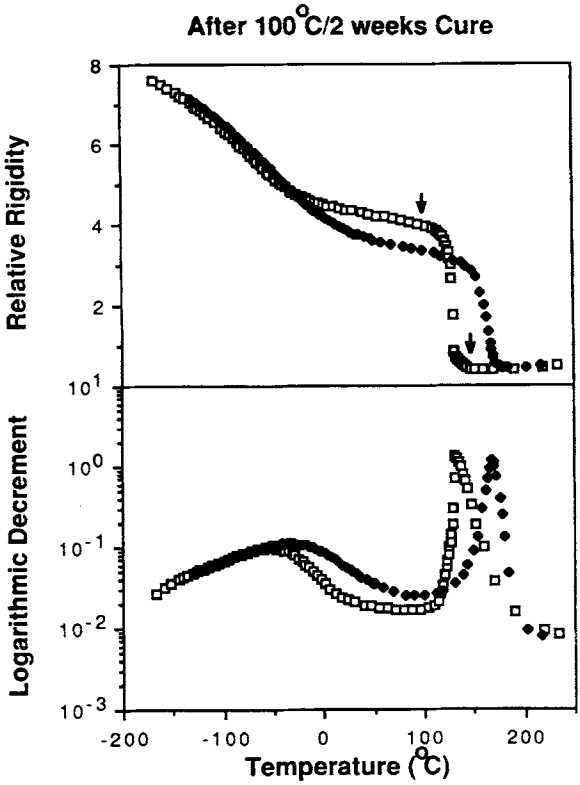

Fig. 10. Dynamic mechanical behavior vs. temperature after 100°C/2 weeks cure: (□) scan from −170 to 240°C after isothermal cure at 100°C for 336 h; (◆) subsequent scan from 240 to −170°C. Vertical arrows indicate the width of the glass transition. Scanning rate: 1.5°C/min in dry helium.

temperature scans to and from 240°C at 1.5°C/min, and (2) thermal degradation reactions compete with cure reactions, especially at high temperatures.

Another relaxation below the glass transition is also apparent in Figure 10; one at approximately −58°C prior to postcure, which has been attributed to the motion of the $-CH_2-CH(OH)-CH_2-O-$ segment which is present in epoxy resins.[26] This glassy-state secondary transition (T_{sec}) increases to −36°C after postcure to 240°C, reflecting the increased steric hindrance associated with further cure.[26] Paradoxically, the findings with respect to the modulus in the glassy state (see below) suggest a larger free volume below T_g to be associated with a higher T_g. Interestingly, for the present epoxy system, the ratio of T_{sec} (K) to T_g (K) remains constant (0.54) and independent of T_g (and of T_c), over the range of T_g's measured, as shown in Figure 11. This suggests that both T_{sec} and T_g are affected and controlled by similar structural factors, such as chemical crosslinks. Data in the literature for other DGEBA systems[2,26] reveal similar results for T_{sec} (K)/T_g (K) (0.56–0.58). The ratio is different for other amorphous polymers [such as polyimides[27]].

As shown in Figure 10, the modulus below the secondary transition appears to be approximately independent of cure, in terms of absolute temperature. This would suggest that the free volume immediately below T_{sec} is indepen-

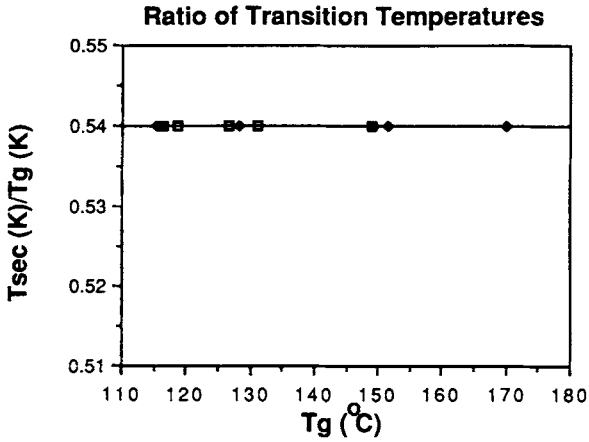

Fig. 11. Ratio of T_{sec} (K)/T_g (K) vs. T_g (°C) at various T_c's: (□) 100°C; (◆) 120°C; (■) 140°C; (◇) 150°C.

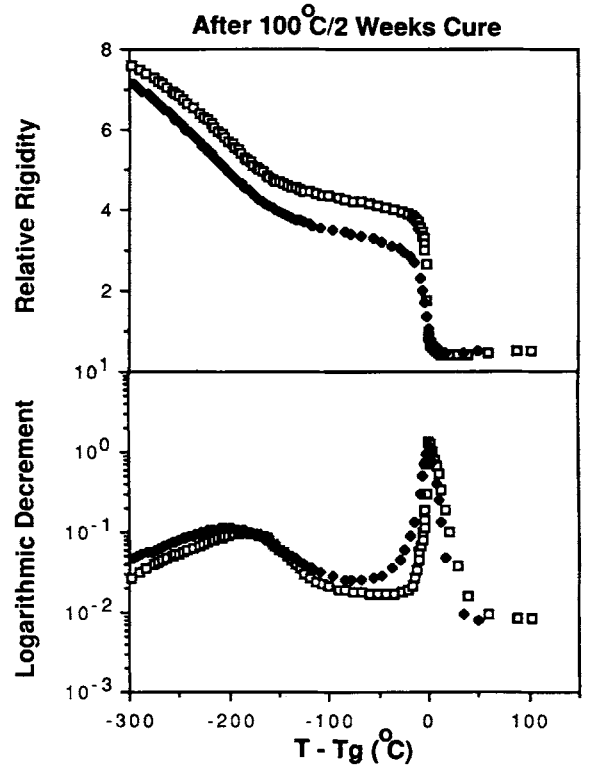

Fig. 12. Dynamic mechanical behavior vs. reduced temperature: (□) scan from −170 to 240°C after isothermal cure at 100°C for 336 h: (◆) subsequent scan from 240 to −170°C. Scanning rate: 1.5°C/min in dry helium.

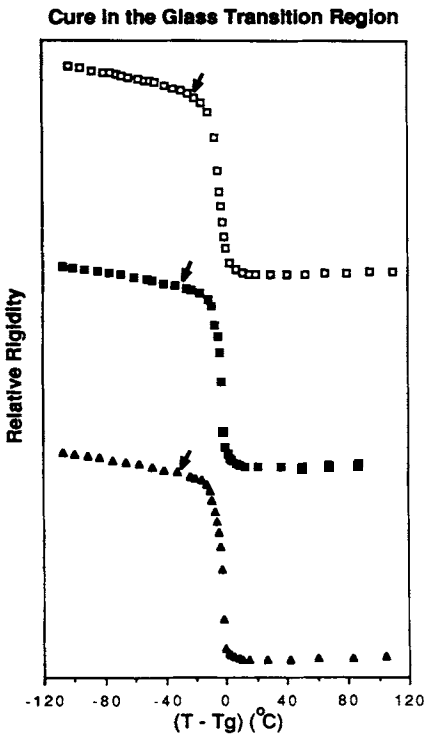

Fig. 13. Cure in the glass transition region. Relative rigidity vs. reduced temperature plots after isothermal cure at 100°C for: (□) 24 h; (■) 70 h; (▲) 7 days. Arrows pinpoint the relative rigidity at $T = T_c$. Scanning rate: 1.5°C/min in dry helium.

dent of cure; yet the free volume level above T_{sec} is dependent upon cure. This apparent contradiction necessitates a more consistent manner for treatment of the data. The data in Figure 10 are replotted vs. reduced temperature ($T - T_g$) in Figure 12. Presented in this manner, the modulus (relative rigidity) level at all temperatures below T_g appears to be controlled by the free volume in the glassy state. On this basis it follows that the similar moduli in the glassy state for $T < T_{sec}$ (Fig. 10) at a given temperature is a coincidence.

Figure 13 shows plots of relative rigidity vs. reduced temperature ($T - T_g$) after isothermal cure at 100°C for various times. Temperature scans were from −170 to 240°C (after cooling from the temperature of cure). The relative rigidity which corresponds to T_c is pinpointed by an arrow on each plot. As the material becomes more glassy during isothermal cure, its T_g increases. This can be a consequence of: (1) chemical aging, as cure is not completely quenched in the glass transition region, and (2) an increase in T_g due to physical annealing during isothermal heating in the glass transition region.[28-31] Figure 14 shows relative rigidity vs. $T - T_g$ plots of materials cured to different extents at T_c = 100, 140, and 170°C, with corresponding T_g's = 130.2, 166.2, and 169.5°C, respectively, as measured during heating scans from −170°C. When the material had vitrified during isothermal cure (T_c = 100 and 140°C), the shape of the transition appears to be similar. In contrast, ΔT_g

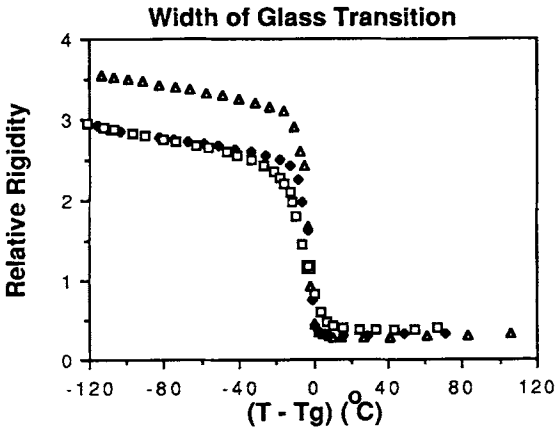

Fig. 14. Width of glass transition. Relative rigidity vs. reduced temperature plots after isothermal cure at T_c: (▲) 100°C, T_g = 130.2°C; (◆) 140°C; T_g = 166.2°C; (□) 169.5°C, T_g = 169.5°C, respectively. Scanning rate: 1.5°C/min in dry helium.

appears to be broader after cure without the occurrence of vitrification. The narrowing of ΔT_g for materials that are cured and vitrified at low T_c's is partly due to physical annealing[11,24,28] (the width of T_g is affected also by conversion). In this study, since T_g is assigned to be close to the rubbery end of the transition (see Fig. 10), the effect of physical annealing on the glass transition temperature will have been removed before T_g is identified by the maximum in the logarithmic decrement. For example, the same value of T_g is obtained (data not shown) during sequential cooling and heating scans for fully cured material. Therefore, the increase in glass transition temperature observed after vitrification is a result of chemical aging rather than physical annealing.

An interesting phenomenon observed in Figures 10 and 14 is that the relative rigidity in the glassy state ($T_g > T > T_{sec}$) decreases with increasing T_g, as has been discussed elsewhere.[2,8,15,24,26,32,33] This anomaly, which is unexpected on the basis that increased chemical crosslinking should lead to higher modulus, has been shown to be associated with corresponding decrease in room temperature (RT ≡ 25°C) density[15,16,24,32-37] and increase in equilibrium level of absorbed water in the glassy state,[15,32] with increasing extent of cure. These anomalies can be linked to a net increase in free volume in the glassy state with increasing conversion. For the present results (Fig. 10), the relative rigidity at RT decreases with increased cure by about 13% (for the same composite specimen), which suggests that

$$G'_p(\mathrm{RT})/G'_{\mathrm{post}}(\mathrm{RT}) = 1.13$$

where $G'_p/(\mathrm{RT})$ and $G'_{\mathrm{post}}/(\mathrm{RT})$ are the moduli of partially and post-cured materials, respectively, at RT.

However, as indicated in eq. (5), the relative rigidity can vary with both the modulus and dimensions of the specimen. If the modulus at RT remains

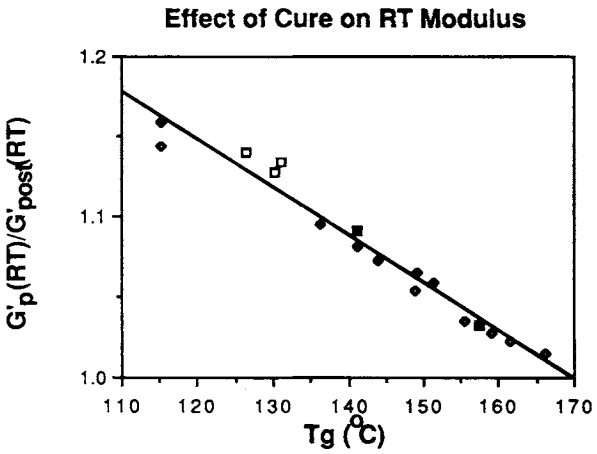

Fig. 15. $G_p'(\mathrm{RT})/G_{\mathrm{post}}'$ (RT) vs. T_g for different isothermal cure temperatures: (□) 100°C; (◆) 120°C; (■) 130°C; (◊) 140°C.

independent of cure, then the relative rigidity can be related to the volume by

$$(1/P^2)_2/(1/P^2)_1 = (V_2/V_1)^{4/3} \tag{6}$$

Hence, the relative rigidity can actually decrease with only volume shrinkage. For the present material, an increase of T_g from 131 to 167.5°C in Figure 10 corresponds to an increase of conversion from ca. 0.92 to ca. 1.0 (see Fig. 22 and later discussion). For the simplicity of discussion, it is assumed that shrinkage varies linearly with conversion during a total shrinkage of 10%. (The latter figure is more than typical for DGEBA systems.[11,38]) A value of V_2/V_1 = ca. 0.99 can then be used in eq. (6), and consequently the relative rigidity, $(1/P^2)$, decreases by about 2% on account of shrinkage due to cure. Therefore, the decrease in relative rigidity of 13% in the glassy state with cure as observed in Figure 10 is due to a similar decrease in the modulus.

As T_g increases from ${}_{\mathrm{gel}}T_g'$ (ca. 67°C) to $T_{g\infty}$ (ca. 170°C), the free volume at RT has been estimated to increase about 20%.[16] This demonstrates the pertinence of free volume in controlling the modulus in the glassy state.[33,39] Figure 15 shows a plot of $G_p'(\mathrm{RT})/G_{\mathrm{post}}'(\mathrm{RT})$ vs. T_g for various T_c's. The data appear to fall on a straight line. (Note that all data points correspond to materials which vitrified and aged during isothermal cure except data points for which T_g = 115°C.) The increase in free volume at RT with increased conversion is the consequence of (1) decreased physical aging efficiency in the glass transition region with increased T_g (i.e., a kinetic basis) and/or (2) increased chemical crosslinking per se (i.e., a structural basis).[15,16,24,32-34,40]

T_g–T_c–Time Relationships

T_g is plotted vs. log time of cure for different isothermal cure temperatures in Figure 16. Also shown are the vitrification and glass (t_{glass}) contours. The former is constructed by locating the points at which $T_g = T_c$: It coincides with that obtained experimentally by isothermal cure (Fig. 9) since T_g and t_{vit}

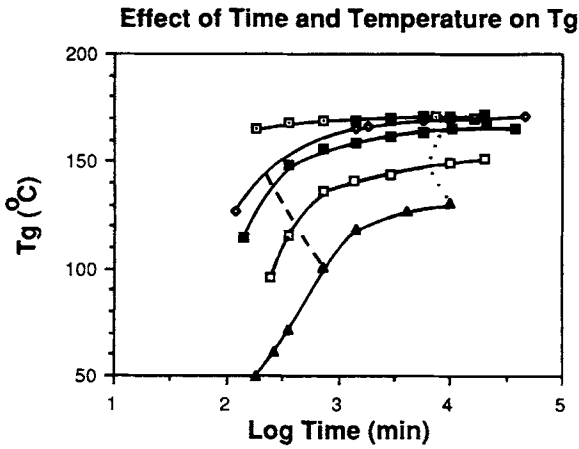

Fig. 16. T_g vs. log time of cure at different isothermal cure temperatures: (▲) 100°C; (□) 120°C; (■) 140°C; (◊) 150°C; (□) 160°C; (◆) 170°C; (⊡) 187°C. Also shown are the vitrification (– – –) and glass (· · ·) curves.

are obtained in a similar fashion (i.e., from maxima in the logarithmic decrement corresponding to the glass transition).

As observed in Figure 16, at low T_c's, T_g increases rapidly during the early stages of cure (which is typical of an nth-order reaction). During the isothermal vitrification process as demarcated by the vitrification and glass curves, T_g increases more slowly with time.[2,38] At high T_c's (ca. $T_{g\infty}$), most of the rise in T_g had occurred prior to the measurements.

The maximum glass transition temperature is ca. 170°C which can be attained by isothermal cure at 160°C for 96 h. However, due to the competition between cure and thermal degradation reactions at high temperatures, it is not obvious whether the glass transition temperature which corresponds to "full" cure is 170°C. Shown in Figure 17 are plots of T_g vs. log time of cure at T_c = 170 and 187°C. The glass transition temperature increases with time and

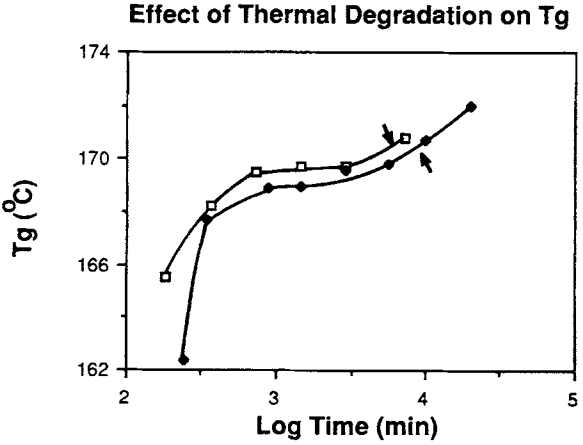

Fig. 17. Effect of thermal degradation on T_g. T_g vs. log time of cure at T_c: (◆) 170°C; (□) 187°C. Arrows indicate times to the onset of char formation.

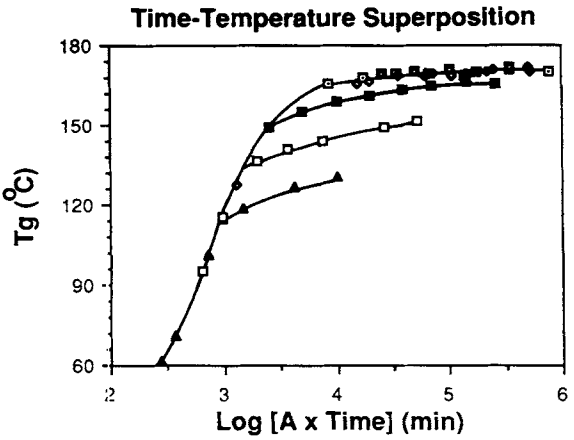

Fig. 18. T_g vs. log (shifted) time of cure at different isothermal cure temperatures (reference temperature = 100°C): (▲) 100°C; (□) 120°C; (■) 140°C; (◊) 150°C; (⊡) 160°C; (◆) 170°C; (□) 187°C.

then levels off at high conversion due to a lower rate of reaction. This is evidence that $T_{g\infty}$ is close to 170°C.[41] After the onset of char formation, as demarcated by the arrows, T_g starts to increase at a faster rate. (An earlier study[14] on the same epoxy system reported a maximum T_g = ca. 172°C).

The T_g curves can be time-shifted using appropriate shift factors A such that the data fall on a master curve at the lower temperature end (Fig. 18). This is based on the assumption that the cure reaction is under only kinetics control at low T_g's (i.e., low conversions where $T_g < T_c$) and that T_g is a direct measure of conversion (see below). Deviations from the composite curve occur when $T_g > T_c$ = 100, 120, and 140°C. This is indicative of diffusion-controlled reactions as the glass transition temperature rises such that T_c is in the glass transition region (see Fig. 13). Similar results have been obtained based on conversion vs. time of cure at different isothermal cure temperatures.[9,42] The shift factors obey an Arrhenius law as shown in Figure 19, giving an activation energy of ca. 15.3 kcal/mol. Similar analysis on T_g's measured by DSC on the

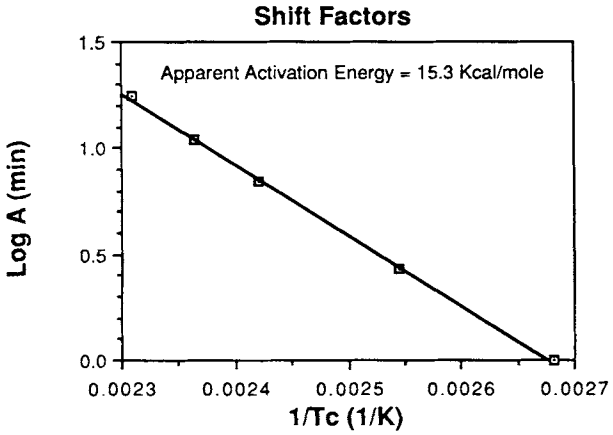

Fig. 19. Arrhenius analysis of the shift factors (A) used in Figure 18.

same epoxy system gave an activation energy (ca. 15 kcal/mol).[16]

T_g as an Index of Cure: Single-Reaction Kinetics Analysis

Let

$$p = \text{degree of conversion}$$

$$r = \text{rate of reaction} = dp/dt = k(T)f(p) \tag{7}$$

where

$$k(T) = \text{Arrhenius rate constant} = A_k \exp(-E/\text{RT}) \tag{8}$$

$$E = \text{activation energy}$$

Substituting eq. (8) into eq. (7) yields

$$dp/dt = A_k \exp[-E/\text{RT}]\, f(p) \tag{9}$$

For isothermal reaction, eq. (9) can be rearranged to yield

$$\int_0^p dp/[A_k f(p)] = \exp[-E/\text{RT}] \int_0^t dt \tag{10}$$

The left-hand side of eq. (10) is a function of p which can be designated $g(p)$ (after integration),

$$\text{and so,} \qquad g(p) = t \exp[-E/\text{RT}] \tag{11}$$

Rearranging eq. (11) and taking the logarithm of both sides,

$$\ln t = E/R(1/T) + \ln g(p) \tag{12}$$

which relates cure time to extent of conversion for each cure temperature ($T = T_c$).

If there is a one-to-one relationship between T_g and p, the function $g(p)$ in eq. (12) will then be a function of T_g only, i.e., $g'(T_g)$. Consequently, plots of ln t vs. $1/T_c$ (K) will give parallel straight lines for each value of T_g, provided that single-reaction kinetics and a one-to-one relationship between T_g and conversion are applicable over the temperature range of interest.

Temperatures and times of cure to obtain the same value of T_g were interpolated from the data in Figure 16. These were then plotted in the form of ln time vs. $1/T_c$ in Figure 20 for values of T_g from 100 to 170°C. Also shown in Figure 20 are the macroscopic gelation, vitrification and glass curves, and the reference temperatures, $T_{g\infty}$ and ${}_{\text{gel}}T_g'$ (ca. 67°C). Cure temperatures from about 100 to 187°C appear to give straight lines up to t_{vit} for each value of T_g. The apparent activation energy calculated from the slope for each value of T_g prior to vitrification increased from 15.3 (at T_g = 100°C) to 16.5 kcal/mol (at T_g = 160°C). [Time-shifted T_g curves for T_g below 100°C also yield an activation energy of 15.3 kcal/mol (see Fig. 19). Also, the apparent

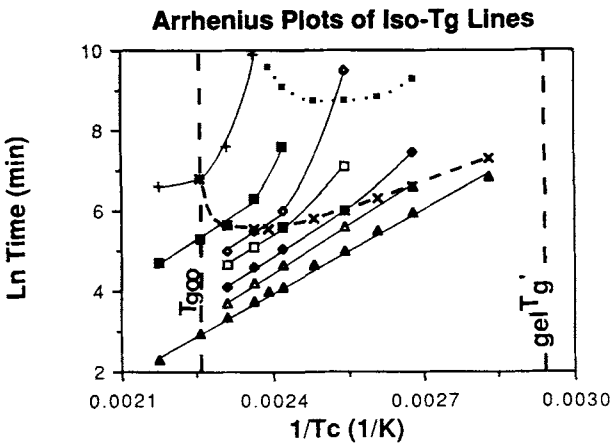

Fig. 20. Arrhenius plots of iso-T_g lines. Ln time vs. $1/T_c$ (1/K) for different values of T_g: (△) 100°C; (◆) 120°C; (□) 140°C; (◇) 150°C; (■) 160°C; (+) 170°C. Other contours shown are: (▲) macroscopic gelation; (X) vitrification (– – –); (■) glass (· · ·).

activation energy as obtained from the times to macroscopic gelation is about ca. 14 kcal/mol (Fig. 20).] From Figure 20, the data start to deviate from a straight line after vitrification (for each value of T_g), which is indicative of diffusion control. The reaction is not diffusion-controlled at t_{vit} due to the manner in which t_{vit} is located (see Fig. 3).

Diffusion Control in the Glass Transition Region

As the glass transition temperature increases beyond the temperature of cure, submolecular mobility plays an important role in the cure of thermosets. Shown in Figure 21 is a plot of log (dT_g/dt) vs. $(-)$ $(T_c - T_g)$ at various T_c's. Cure reactions to the right of the dashed line (i.e., $T_c = T_g$) proceed in the glass transition region. At $T_c = 100$ and 120°C, the reaction rates appear to be identical when $T_g \geq T_c + 20$°C. This is indicative of the same type of physical

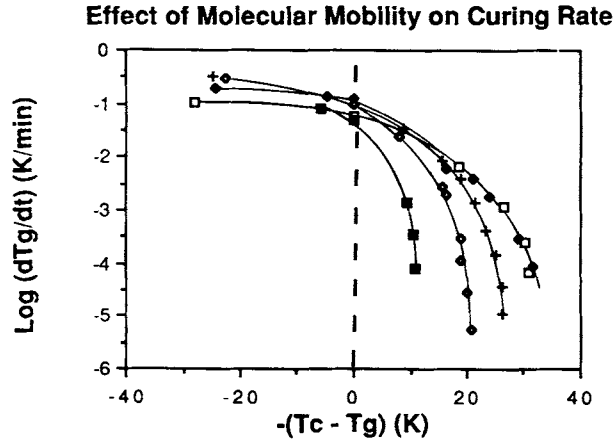

Fig. 21. Effect of molecular mobility on curing rate. Log dT_g/dt) vs. $-(T_c - T_g)$ at various T_c's: (□) 100°C; (◆) 120°C; (+) 140°C; (◇) 150°C; (■) 160°C.

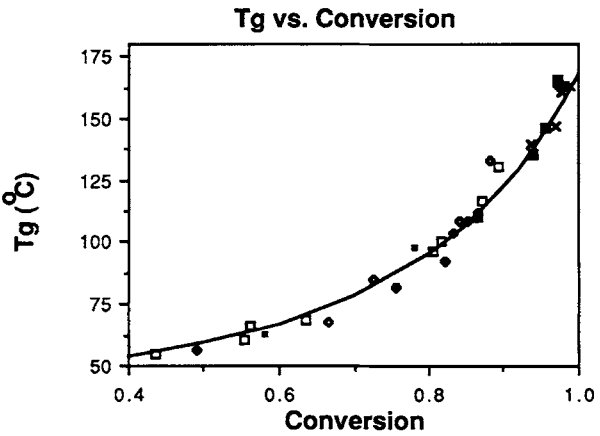

Fig. 22. T_g vs. conversion at various T_c's using DSC data[24]: (■) 66.7°C; (◆) 80°C; (□) 100°C; (◊) 120°C; (■) 140°C; (X) 165°C; (+) 180°C.

relaxation process being in contol at the end of the glass transition region. At T_c = 160°C, the rapid dropoff in reaction rates is due to chemical control at high conversions. For T_cs between 120 and 160°C, the reaction rates are affected by a combination of kinetics control because of high conversions, and of diffusion control.

It has been suggested[43] that the following modified WLF equation[44] can be applied to study the cure of thermosets in the diffusion controlled region

$$\log(dT_g/dt) = K - ab/[b + (T_c - T_g)] \tag{13}$$

where K, a, and b are constants. This expression should apply well after vitrification. The experimental limiting value of $(T_c - T_g)$ is about -32 K whereas the corresponding limit for eq. (13) is -50 K.

In order to obtain information about the rate constants in the glass transition region, experimental values of conversion vs. T_g are needed. A plot of T_g vs. extent of cure for the present system is shown in Figure 22. The degree of cure was obtained from the residual exotherm of a partially cured specimen in comparison with the total heat of reaction of an unreacted sample, as measured by DSC at 10°C/min.[16,24] Note that the value for $T_{g\infty}$ = 168°C was obtained using DSC. For the present discussion, a value of $T_{g\infty}$ = 170°C is used. Employing a modified version of an empirical equation which is available in the literature,[45] T_g can be related to the degree of cure, p, as follows:

$$1/T_g = (1 - p)/T_{g0} + p/T_{g\infty} + p(1 - p)(0.0026p - 0.0008) \tag{14}$$

The solid curve in Figure 22 corresponds to eq. (14). T_g increases more rapidly with conversion after p = ca. 0.7, which probably corresponds to macroscopic gelation. This is different from the theoretical value of 0.577 for molecular

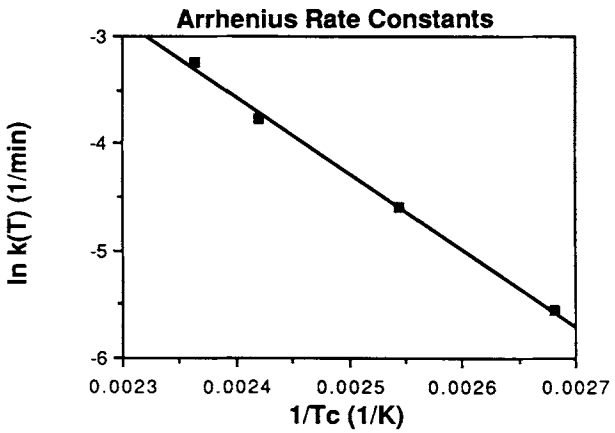

Fig. 23. Arrhenius rate constants. ln $k(T)$ vs. $1/T_c$ in the absence of diffusion control.

gelation for a system with a branching unit of functionality[23] 4 due to unequal reactivity of the primary and secondary amines with epoxy groups,[2] intramolecular reactions which do not increase molecular weight, and the macroscopic method for assigning gelation.

Analysis of the conversion data for low conversions in the absence of diffusion control (not shown here), for both isothermally and nonisothermally (10°C/min) cured specimens, indicates that the reaction order is ca. 1.5.[24] Hence, eq. (7) can be given more generally as

$$dp/dt = k(T, p)(1 - p)^{1.5} \tag{15}$$

Here, the rate constant $k(T, p)$ can be a function of conversion when under combined chemical and diffusion control.[45,46] Assuming the reaction mechanism is independent of diffusion control,[46] the observed rate constant $k(T, p)$ can be calculated using eq. (15). Prior to vitrification, the rate constants due to chemical control obey an Arrhenius law and are shown in Figure 23 [vs. $1/T_c$ (K)]. From the slope of the straight line, an activation energy of 14.2 kcal/mol is obtained. This value is similar to those obtained from Figures 18–20 (i.e., 15–16.5 kcal/mol). All of the computed rate constants are plotted vs. conversion in Figure 24. The solid arrows indicate the conversions at which $T_g = T_c$. Notice that the rate constants decrease rapidly after the vitrification point.

The Isothermal TTT Diagram with Iso-T_g Contours

The iso-T_g contours in Figure 20 are replotted in the form of T_c vs. log time of cure in the form of a TTT cure diagram in Figure 25. The set of iso-T_g contours depicts the approach of the reaction towards completion. Similar information can also be obtained from iso-conversion curves which have been measured using spectroscopic, e.g., infrared,[2] techniques. However, such conventional techniques would appear to be less sensitive at high conversion for measuring the change in degree of cure with time, since, as shown in Figure 22, T_g increases more rapidly with conversion during the later stages of cure. This has been explained in terms of the T_g being dominated by the population of

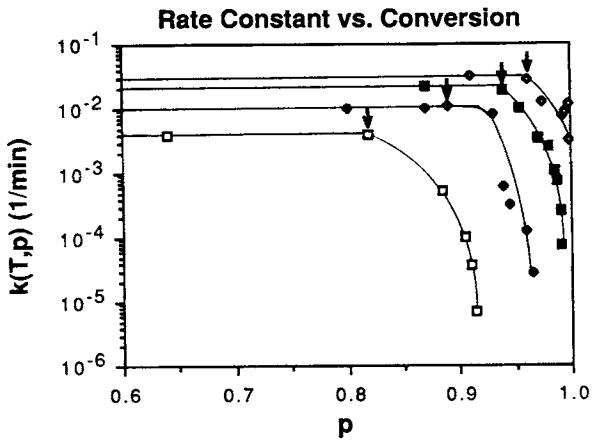

Fig. 24. $k(T, p)$ vs. p at various T_c's: (□) 100°C; (◆) 120°C; (■) 140°C; (◊) 150°C.

the highest crosslinked junctions which appear after gelation.[16] The glass transition temperature, as a parameter by itself, is more informative in terms of material behavior and is easier to obtain than the degree of conversion, particularly in the later stages of cure (e.g., conversion > 95%).

In Figure 25, it can be observed that the "window" for cure to achieve maximum cure, between the $T_g = 170°C$ contour and the char formation contour for $T_c > T_{g\infty}$, is limited. For $T_c < T_{g\infty}$, the "window" is further defined by the maximum relative rigidity contour. Consequently, the intrinsic T_g at full cure may not be realized by an isothermal cure process for high T_g epoxy systems. For circumstances in which the crosslink density of the cured epoxy material is of major concern, it is necessary to obtain material with the highest crosslink density (i.e., T_g) without degradation. The iso-T_g lines coupled with the TTT cure diagram (Fig. 25) can provide a tool for selecting a proper isothermal cure path to obtain a maximum value of T_g.

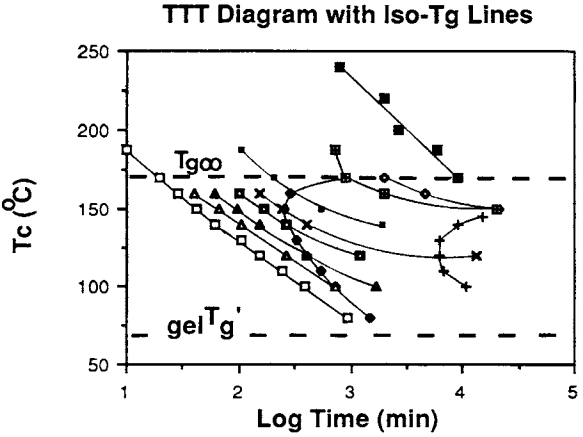

Fig. 25. Time–temperature–transformation (TTT) cure diagram iso-T_g contours: (△) 100°C; (▲) 120°C; (□) 140°C; (X) 150°C; (■) 160°C; (⊞) 170°C. Other contours shown are: (□) macroscopic gelation; (◆) vitrification; (+) glass; (◊) maximum relative rigidity; (■) char formation.

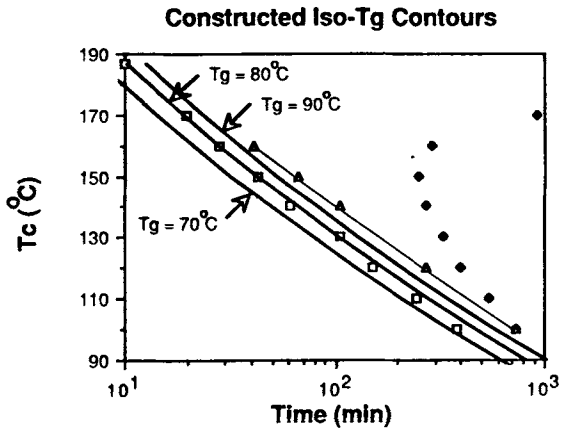

Fig. 26. Calculated iso-T_g curves for 70, 80, and 90°C, in the form of an isothermal TTT cure diagram which includes experimental (□) macroscopic gelation, (◆) vitrification, and (▲) T_g = 100°C contours. Notice that the macroscopic gelation curve lies between T_g = 70 and 80°C curves.

At isothermal vitrification, eq. (12) can be rewritten as

$$\ln t_{vit} = E/R(1/T_g) + \ln g'(T_g) \tag{16}$$

as $T_g = T_c$. For isoconversion, ln $g'(T_g)$ is constant. Hence, combining eqs. (12) and (16), and rearranging yields

$$t = t_{vit} \exp\left[E/R(1/T_c - 1/T_g)\right] \tag{17}$$

which can be used to construct iso-T_g contours (i.e., T_c vs. time of cure to obtain a particular value of T_g)[47] given the value of E, t_{vit}, and T_g. In the following example E = 15 kcal/mol was used, which is that obtained from time–temperature superposition (Fig. 18) and single-reaction kinetics analyses (Fig. 20) for T_g < 100°C. To construct iso-T_g contours for T_g = 70, 80, and 90°C, the corresponding t_{vit} values are also needed. These were obtained experimentally for T_c = 80 and 90°C (Fig. 9) and by extrapolation for T_c = 70°C [using a plot of log t_{vit} vs. $1/T_c$ (K)]. The constructed iso-T_g contours according to eq. (17) are shown in Figure 26. Also shown are the experimental macroscopic gelation, vitrification, and experimental T_g = 100°C contours. The macroscopic gelation curve appears to cross the T_g = 70 and 80°C curves; it probably corresponds to an isoviscous contour.

CONCLUSIONS

Isothermal vitrification, which occurs during cure below the maximum glass transition temperature ($T_{g\infty}$) of a cured epoxy system, can cause the reactions to become diffusion-controlled, thereby limiting the degree of conversion. Consequently, high temperatures of cure are often necessary to attain "full" cure for high T_g epoxy systems. Thermal degradation reactions can compete with cure at high temperatures.

The glass transition temperature of a diglycidyl ether of bisphenol A cured with a tetrafunctional aromatic diamine has been investigated (using principally torsional braid analysis) as a function of time and temperature (T_c) of isothermal cure, in an attempt to achieve "full" cure without thermal degradation (maximum $T_g \geq 171°C$).

Thermal degradation can cause the modulus at T_c to pass through a maximum when cured below $T_{g\infty}$. For $T_c > T_{g\infty}$, "char" formation can cause the modulus to increase on further heating after reaching a plateau.

The modulus in the glassy state below T_g is observed to decrease with increasing conversion. This anomaly, which is associated with a net increase in free volume in the glassy state, arises either as a consequence of chemical crosslinking and/or from physical annealing being more efficient in the glass transition region at lower conversions (i.e., lower T_g's).

The ratio of T_{sec} (K)/T_g (K) is observed to be constant. This suggests that both transition temperatures are controlled by similar structural factors, such as chemical crosslinks.

Analysis of T_g data based on single-reaction kinetics and time–temperature superposition reveals the merit of using the glass transition temperature as an index of progress of cure. T_g is a sensitive indicator as it increases more rapidly with increasing conversion in the final stages of cure.

An approach leading to a series of iso-T_g lines on a time–temperature–transformation (TTT) cure diagram, which can be used to design time–temperature isothermal cure paths leading to particular values of T_g, is described.

Financial support has been provided by the Office of Naval Research.

References

1. J. K. Gillham, in *Developments in Polymer Characterisation*—3, J. V. Dawkins, Ed., Applied Science, London, 1982, Chap. 5, pp. 159–227.

2. J. B. Enns and J. K. Gillham, *J. Appl. Polym. Sci.*, **28**, 2567 (1983).

3. Y. Tanaka and T. J. Mika, in *Epoxy Resins, Chemistry and Technology*, C. A. May and Y. Tanaka, Eds., Dekker, New York, 1973, Chap. 3.

4. K. Dusek, M. Bleha and S. Lunak, *J. Polym. Sci., Polym. Chem. Ed.*, **15**, 2393 (1977).

5. N. S. Schneider, J. F. Sprouse, G. L. Hagnauer, and J. K. Gillham, *Polym. Eng. Sci.*, **19**, 304 (1979).

6. L. H. Lee, *J. Polym. Sci., A*, **3**, 859 (1965).

7. S. C. Lin, B. J. Bulkin, and E. M. Pearce, *J. Polym. Sci., Polym. Chem. Ed.*, **17**, 3121 (1979).

8. L. C. Chan, H. N. Nae, and J. K. Gillham, *J. Appl. Polym. Sci.*, **29**, 3307 (1984).

9. S. Lunak, J. Vladyka, and K. Dusek, *Polymer*, **19**, 931 (1978).

10. B. A. Rozenberg, *Epoxy Resins and Composites II*, K. Dusek, Ed., Advances in Polymer Science, Vol. 75, Springer-Verlag, New York, 1986, pp. 113–165.

11. E. F. Oleinik, *Epoxy Resins and Composites IV*, K. Dusek, Ed., Advances in Polymers Science, Vol. 80, Springer-Verlag, New York, 1986, pp. 49–99.

12. J. B. Enns and J. K. Gillham, *Amer. Soc., Adv. Chem. Ser.* **203**, 27 (1983).

13. X. Peng and J. K. Gillham, *J. Appl. Polym. Sci.*, **30**, 4685 (1985).

14. K. P. Pang and J. K. Gillham, *Proc. Am. Chem. Soc., Div. Polym. Mater. Sci. Eng.*, **55**, 64 (1986).

15. M. T. Aronhime, X. Peng, and J. K. Gillham, *J. Appl. Polym. Sci.*, **32**, 3589 (1986).

16. K. P. Pang and J. K. Gillham, *Proc. Am. Chem. Soc., Div. Polym. Mater. Sci. Eng.*, **56**, 435 (1987); *J. Appl. Polym. Sci.*, **37**, 1969 (1989).

17. C. Y. M. Tung and P. J. Dynes, *J. Appl. Polym. Sci.*, **27**, 569 (1982).
18. D. Harran and A. Laudouard, *J. Appl. Polym. Sci.*, **32**, 6043 (1986).
19. F. Chambon, Z. S. Petrovic, W. J. MacKnight, and H. H. Winter, *Macromolecules*, **19**, 2146 (1986).
20. D. Katz and A. V. Tobolsky, *Polymer*, **4**, 417 (1963).
21. G. A. Pogany, *Eur. Polym. J.*, **6**, 343 (1970).
22. M. Shen, T. Y. Chen, E. H. Cirlin, and H. M. Gebhard, *Polymer Networks, Structure and Mechanical Properties*, A. J. Chompff and S. Newman, Eds., Plenum, New York, 1971, pp. 47–56.
23. P. J. Flory, *Principles of Polymer Chemistry*, Cornell University Press, Ithaca, NY, 1953.
24. K. P. Pang, Ph.D. dissertation, Department of Chemical Engineering, Princeton University, 1988.
25. P. G. Babayevsky and J. K. Gillham, *J. Appl. Polym. Sci.*, **17**, 2067 (1973).
26. G. A. Pogany, *Polymer*, **11**, 66 (1970).
27. J. K. Gillham and H. C. Gillham, *Polym. Eng. Sci.*, **13** (6), 447 (1973).
28. R. A. Fava, *Polymer*, **9**, 137 (1968).
29. Z. H. Ophir, J. A. Emerson, and G. L. Wilkes, *J. Appl. Phys.*, **49**, 5032 (1978).
30. E. S. W. Kong, *Epoxy Resins and Composites IV*, K. Dusek, Ed., Advances in Polymers Science, Vol. 80, Springer-Verlag, New York, 1986, pp. 125–172.
31. J. Mijovic and K. F. Lin, *J. Appl. Polym. Sci.*, **32**, 3211 (1986).
32. J. B. Enns and J. K. Gillham, *J. Appl. Polym. Sci.*, **28**, 2831 (1983).
33. A. Noordam, J. J. M. H. Wintraecken, and G. Walton, *Crosslinked Epoxies*, B. Sedlacek and J. Kahovec, Eds., de Gruyter, New York, 1987, pp. 373–389.
34. A. Shimazaki, *J. Polym. Sci., C*, **23**, 555 (1968).
35. W. Fisch, W. Hofman, and R. Schmid, *J. Appl. Polym. Sci.*, **13**, 295 (1969).
36. K. Suzuki, Y. Miyano, and T. Kunio, *J. Appl. Polym. Sci.*, **21**, 3367 (1977).
37. D. A. Shimp, *Proc. Am. Chem. Soc., Div. Polym. Mater., Sci. Eng.*, **54**, 107 (1986).
38. I. C. Choy and D. J. Plazek, *J. Polym. Sci., Polym. Phys. Ed.* **24**, 1303 (1986).
39. R. N. Haward, *The Physics of Glassy Polymers*, R. N. Haward, Ed., Applied Science, London, 1973.
40. J. K. Gillham, *Polym. Eng. Sci.*, **19**, 676 (1979).
41. G. R. Palmese and J. K. Gillham, *J. Appl. Polym. Sci.*, **34**, 1925 (1987).
42. M. J. Acitelli, R. B. Prime, and E. Sacher, *Polymer*, **12**, 333 (1971).
43. M. Gordon and W. Simpson, *Polymer*, **2**, 383 (1961).
44. M. L. Williams, R. F. Landel, and J. D. Ferry, *J. Am. Chem. Soc.*, **77**, 3701 (1955).
45. I. Havlicek and K. Dusek, *Crosslinked Epoxies*, B. Sedlacek and J. Kahovec, Eds., de Gruyter, New York, 1987, pp. 417–424.
46. F. G. A. E. Huguenin and M. T. Klein, *Ind. Eng. Chem., Prod. Res. Dev.*, **24**, 166 (1985).
47. S. Gan, J. K. Gillham, and R. B. Prime, *J. Appl. Polym. Sci.*, **37**, 803 (1989).

Received August 29, 1988
Accepted October 24, 1988